Journal of Nuclear Materials 395 (2009) 162–168

Contents lists available at ScienceDirect

Journal of Nuclear Materials

journal homepage: www.elsevier.com/locate/jnucmat

Review

Interdiffusion between U(Mo,Pt) or U(Mo,Zr) and Al or Al A356 alloy

C. Komar Varela [a,b], M. Mirandou [a,b,*], S. Aricó [b], S. Balart [b], L. Gribaudo [b,c]

[a] Instituto Sabato – UNSAM-CNEA, Av. Gral. Paz 1499, B1650KNA, San Martín, Argentina
[b] Departamento Materiales, GIDAT-GAEN-CNEA, Av. Gral. Paz 1499, B1650KNA, San Martin, Argentina
[c] Consejo Nacional de Investigaciones Científicas y Tecnológicas, Avda. Rivadavia 1917, C1033AAJ, Buenos Aires, Argentina

ARTICLE INFO

Article history:
Received 9 January 2009
Accepted 9 October 2009

PACS:
28.50.Dr
61.10.Nz
66.30.Ny

ABSTRACT

Solid state reactions in chemical diffusion couples U–7 wt.%Mo–0.9 wt.%Pt/Al at 580 °C and U–7 wt.%Mo–0.9 wt.%Pt/Al A356 alloy, U–7 wt.%Mo–1 wt.%Zr/Al and U–7 wt.%Mo–1 wt.%Zr/Al A356 alloy at 550 °C were characterized. Results were obtained from optical and scanning electron microscopy, electron probe microanalysis and X-ray diffraction. The UAl_3, UAl_4 and $Al_{20}Mo_2U$ phases were identified in the interaction layers of γU(Mo,Pt)/Al and γU(Mo,Zr)/Al diffusion couples. $Al_{43}Mo_4U_6$ ternary compound was also identified in γU(Mo,Zr)/Al due to the decomposition of γU(Mo,Zr) phase.

The $U(Al,Si)_3$ and U_3Si_5 phases were identified in the interaction layers of γU(Mo,Pt)/Al A356 and γU(Mo,Zr)/Al A356 diffusion couples. These phases are formed due to the migration of Si to the interaction layer. In the diffusion couple U(Mo,Zr)/Al A356, Zr_5Al_3 phase was also identified in the interaction layer.

The use of synchrotron radiation at Brazilian Synchrotron Light Laboratory (LNLS, CNPq, Campinas, Brazil) was necessary to achieve a complete crystallographic characterization.

Contents

1. Introduction

The use of low enriched uranium in γU(Mo) alloys is under study in dispersion or monolithic fuel elements to convert high flux research nuclear reactors [1,2]. A *dispersion fuel element* consists of a meat formed by a mixture of powders of an U(Mo) alloy

* Corresponding author. Address: Instituto Sabato – UNSAM-CNEA, Av. Gral. Paz 1499, B1650KNA, San Martín, Argentina. Tel.: +54 11 6772 7222; fax: +54 11 6772 7362.
E-mail address: mirandou@cnea.gov.ar (M. Mirandou).

0022-3115/$ - see front matter © 2009 Elsevier B.V. All rights reserved.
doi:10.1016/j.jnucmat.2009.10.050

(in the cubic γU phase, cI2, W *type*) and pure Al, cladded with an Al alloy. As fabrication process and irradiation favour the interdiffusion between U(Mo) and Al, which may give rise to a detrimental interaction layer, several *in pile* and *out of pile* investigations are in process as part of the γU(Mo) qualification. Pos irradiation experiments have shown a significant interaction layer producing a considerable swelling and, in some cases, an unacceptable porosity located in the interface interaction layer/Al [3–7]. This porosity is related to a poor irradiation behavior of the phases that form this interaction layer [4,8]. *Out of pile* experiments have been an important tool as a first approximation to understand and solve this problem [9–13]. In brief, results obtained by several authors in diffusion couples γU(Mo)/Al at high temperatures (500–600 °C), have shown that UAl_3 (cP4), UAl_4 (oI20) and $Al_{20}Mo_2U$ (cF184) phases form the interaction layer [9–11]. Being a metastable phase, γU can decompose into Mo-rich γU phase (γ′U) + orthorhombic αU phase, oC4, with lamellar cellular-like morphology. When this happens, the interaction layer grows abruptly and the ternary compound $Al_{43}Mo_4U_6$ (hP106) is also identified [10,13,14]. It is known that a small amount of Pt added to γU(Mo) is efficient in retaining γU phase at high temperature [15]. Nevertheless, no information was found in the literature related to the influence of Pt in the interaction layer.

The addition of Si to Al and/or Zr to U(Mo) was proposed, and are currently being studied, as possible solutions to reduce the interaction layer or alter it composition [4,16,17]. Experiments performed by different authors on diffusion couples U(Mo)/Al(Si) [14,16–23] showed, in good agreement, that Si migrates to and concentrates in the interaction layer. A precipitate free zone (PFZ) also appears in the component Al(Si) in a zone contiguous to the interaction layer due to the dissolution of Si precipitates. A complete crystallographic characterization of the interaction layer in the diffusion couples U–7 wt.%Mo/Al A356 (7.1 wt.%Si) [18] and U–7 wt.%Mo/Al 6061 (0.6 wt.%Si) [14] showed that $U(Al,Si)_3$ (cP4, Cu_3Au *type*) and the hexagonal U_3Si_5 (hP3, AlB_2 *type*) are the phases formed due to the migration of Si to the interaction layer. In Ref. [23] authors conclude that Zr added to U(Mo) and Si added to Al had similar effects on reducing the interaction layer growth and also remark that Zr is most effective in combination with Si added to Al. It is also concluded that the interaction product formed at or near the U(Mo,Zr)/interaction layer interface has the Al/(U + Mo) ratio of ~2 but no information about the crystalline structures of the phases that are part of interaction layer is presented.

This work presents results of *out of pile* interdiffusion experiments in couples U–7 wt.%Mo–0.9 wt.%Pt/Al at 580 °C and U–7 wt.%Mo–0.9 wt.%Pt/Al A356 alloy, U–7 wt.%Mo–1 wt.%Zr/Al and U–7 wt.%Mo–1 wt.%Zr/Al A356 alloy at 550 °C. Phase characterization of each interaction layer was achieved by the combined analysis of composition determination together with crystalline structure identification. The use of synchrotron radiation at the Brazilian Synchrotron Light Laboratory (LNLS, CNPq, Campinas, Brazil) was necessary to achieve a complete crystallographic characterization.

2. Experimental procedure

Three different U-base alloys were made with the following compositions: U–7 wt.%Mo [U(Mo)], U–7 wt.%Mo–0.9 wt.%Pt [U(Mo,Pt)] and U–7 wt.%Mo–1 wt.%Zr [U(Mo,Zr)]. They were fabricated by arc melting in a small non-consumable tungsten electrode arc-furnace with a copper crucible under pure argon atmosphere. Depleted U (0.2 at.% ^{235}U with principal impurities 27 wppm Fe, 60 wppm Mg, 24 wppm Si and <10 wppm Al); Mo 99.97% (<20 wppm O_2, <10 wppm N_2, <10 wppm C, <100 wppm W, 8 wppm Si and 2 wppm Ni); Pt 99.95% and Zr 99.85% (420 wppm O_2 and <170 wppm Fe) were used. Samples in the as-cast condition were sealed into quartz tubes under pure Ar atmosphere, homogenized in composition by an isothermal treatment of 2 h at 1000 °C and quenched in water without tube breaking to retain γU phase in metastable condition.

Pure Al 99.99% and the commercial Al A356 alloy (provided by Aluar S.A.) were used. This alloy (principal impurities: 7.1 wt.%Si, 0.37 wt.%Mg, 0.12 wt.%Ti, 0.10 wt.%Fe, 0.02 wt.%Zn, 0.01 wt.%Ca, 0.001 wt.%Sr) was used as provided by the manufacturer. In this condition, most of the Si present in the Al alloy forms needle-shaped pure Si precipitates that are located in the Al grain boundaries.

Seven diffusion couples were made mechanically pressing plates of approximately $(2 \times 5 \times 5)\ mm^3$, cut from the different alloys, using stainless steel clamps. The diffusion couples were sealed into quartz tubes under Ar atmosphere, isothermally treated and quenched in water without tube breaking. Details are shown in Table 1.

Two different configurations of diffusion couples were built, Table 1. One of them (samples *II*, *IV*, *VI* and *VII*) was made to characterize a single interaction layer by XRD. Successive surfaces, at different depths, were exposed by polishing parallel to the diffusion front. The other configuration (multicouples *I*, *III* and *V*), was made to characterize and compare different interaction layers grown simultaneously [21]. In this case, multicouples were cut perpendicular to the diffusion front, Fig. 1. Samples of both configurations were suitably grinded and mechanically polished up to 1 μm diamond paste. In some cases a HF 1% v/v final chemical etching was used to reveal the interaction layer microstructure.

Phase characterization was performed by Optical Microscopy (OM – Olympus BX60 M), Scanning Electron Microscopy (SEM – Philips SEM 515), Wavelength Dispersive Spectroscopy (WDS – CAMECA SX50) against standards and X-ray Diffraction with a conventional diffractometer (XRD – Philips PW3710) and with synchrotron radiation (XRD – XRD1 line at the Brazilian Syncrotron Light Laboratory – LNLS).

Interaction layer widths were measured with an eye-piece micrometer (appreciation ±1 μm). For each one, ten values were taken at different points of the interaction layers. As some of these presented irregular interfaces, the criterion adopted in this paper is to consider the minimum and maximum value measured for each one and to present it as a range.

Table 1
Diffusion anneal details and characterization techniques.

Sample	Couple	*T* (°C)	Time (h)	Characterization technics
I	U(Mo,Pt)/Al/U(Mo)	580	2	OM; WDS
II	U(Mo,Pt)/Al			XRD^{cd}
III	U(Mo,Pt)/Al A356/U(Mo)	550	1.5	OM; WDS
IV	U(Mo,Pt)/Al A356			XRD^{cd}
V	U(Mo,Zr)/Al/U(Mo)/Al A356/U(Mo,Zr)			OM; SEM; WDS
VI	U(Mo,Zr)/Al			XRD^{cd} XRD^{sr}
VII	U(Mo,Zr)/Al A356			XRD^{cd} , XRD^{sr}

XRD^{cd} = XRD with a conventional diffractometer.
XRD^{sr} = XRD with synchrotron radiation.

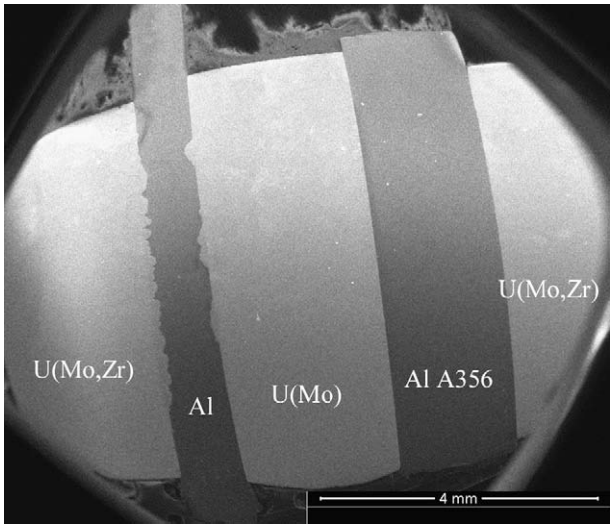

Fig. 1. Sample *V*. 550 °C-1.5 h. Image of multicouple. SEM, mechanical polishing.

The quantitative compositional microanalysis by WDS was made under an accelerating potential of 20 kV. The equipment was recalibrated before each analysis session using pure Al, Mo, Si, U and Pt (or Zr) standards.

XRD measurements with conventional diffractometer were performed at room temperature with filtered Cu Kα radiation, $\lambda = 0.1540$ nm. When synchrotron radiation was used, an energy of 8.014 keV was selected resulting in $\lambda = 0.1547$ nm obtained by the use of the LaB_6 diffraction pattern. In both cases, powder diffraction technique was applied to bulk samples. Crystalline structure identification and the estimation of the lattice parameters were obtained by the use of the PowderCell program [24]. This program is a very useful tool because it allows the confirmation of the presence or absence of a phase by a visual comparison between the individual theoretical spectrum of any phase and the experimental one. The lattice parameter estimation was done in the same way.

3. Results

After the diffusion anneals an interaction layer was observed between the U-base alloys and the Al or Al A356 on the seven samples described in Table 1. In the Al A356 alloy, in a zone contiguous to the interaction layer, a PFZ appeared due to the dissolution of Si precipitates (Samples *III*, *IV*, *V* and *VII*).

3.1. Morphology of the interaction layers

3.1.1. U(Mo,Pt)/Al

On sample *I* (580 °C-2 h), U(Mo,Pt) and U(Mo) alloys retained metastable γU phase. Interaction layers γU(Mo)/Al and γU(Mo,Pt)/Al showed planar interfaces and almost constant widths. Values of interaction layers ranged from 103 to107 μm for U(Mo)/Al and from 77 to 85 μm for U(Mo,Pt)/Al, Fig. 2a and b. Chemical etching revealed the existence of different zones inside both interaction layers.

3.1.2. U(Mo,Zr)/Al

On sample *V* (550 °C-1.5 h), U(Mo,Zr) and U(Mo) alloys presented isolated areas where γU phase decomposed, with lamellar cellular-like morphology, into αU and γ′U phases. Comparing both alloys, a greater amount of these areas was observed in U(Mo,Zr) alloy. Concerning interaction layers with pure Al, both of them presented very irregular interfaces, Fig. 3. Widths of the U(Mo,Zr)/Al interaction layer took values from 12 to 150 μm while those for U(Mo)/Al interaction layer did from 8 to 210 μm.

3.1.3. U(Mo,Pt)/Al A356

On sample *III* (550 °C-1.5 h), the U(Mo,Pt) alloy retained γU phase while the U(Mo) alloy presented isolated areas where γU phase decomposed with lamellar cellular-like morphology. Although this difference in the crystallographic state of the U-base alloys, both interaction layers showed planar interfaces and almost constant widths being the measured values 15–25 μm for U(Mo,Pt)/Al A356 and 20–25 μm for U(Mo)/Al A356 (Fig. 4).

3.1.4. U(Mo,Zr)/Al A356

On sample *V* (550 °C-1.5 h), as mentioned in 3.1.2., U(Mo,Zr) and U(Mo) alloys presented isolated areas where γU phase decomposed. However, interaction layers with Al A356 showed planar

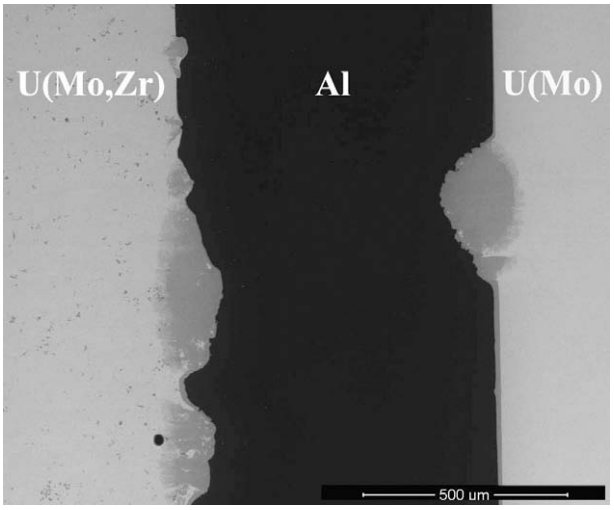

Fig. 3. Sample *V*. 550 °C-1.5 h. Interaction layers with very irregular interfaces in U(Mo,Zr)/Al/U(Mo). SEM, mechanical polishing.

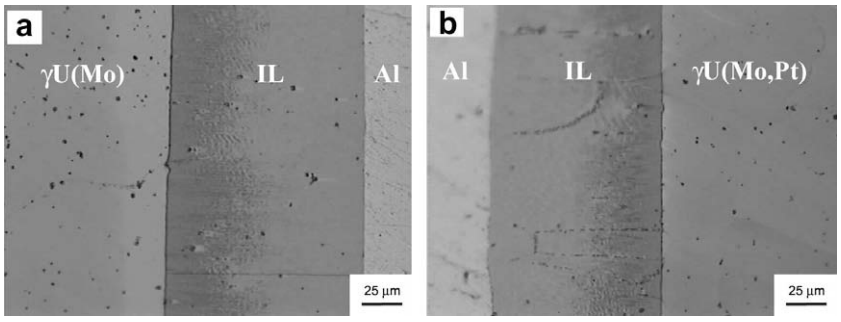

Fig. 2. Sample *I*. 580 °C-2 h. Interaction layers with planar interfaces in: (a) γU(Mo)/Al and (b) γU(Mo,Pt)/Al. OM, chemical etching. IL stands for Interaction Layer.

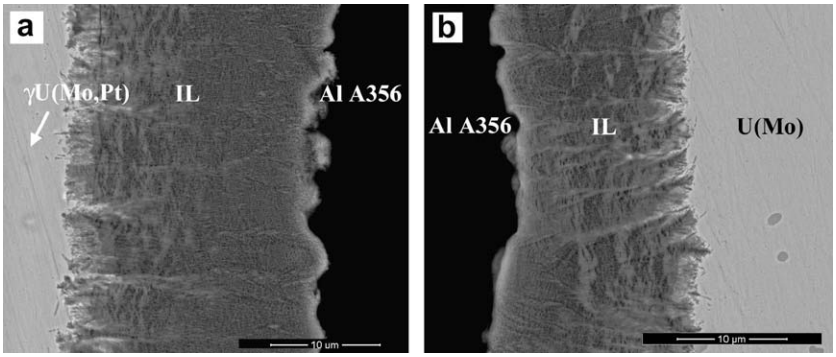

Fig. 4. Sample *III*. 550 °C-1.5 h. Interaction layer with planar interfaces in: (a) γU(Mo,Pt)/Al A356, (b) U(Mo)/Al A356. BSE-SEM, mechanical polishing. IL stands for Interaction Layer.

interfaces and almost constant widths, similar to U(Mo,Pt)/Al A356 behavior (see Fig. 4). Values measured for U(Mo,Zr)/Al A356 ranged from 4 to 8 μm while U(Mo)/Al A356 did from 8 to 12 μm.

At this point, it is important to note that thickness ranges for U(Mo)/Al A356 gathered from samples III (see Section 3.1.3) and V (this section) present some difference. As two different samples are involved, we consider that this difference is acceptable and the criteria adopted in this paper to compare the thickness of the interaction layers is to do it only with interaction layers belonging to the same sample (i.e. same experimental conditions).

3.2. Phase identification

Composition measurements and X-ray diffraction were used to identify the phases present in the different interaction layers.

3.2.1. U(Mo,Pt)/Al

Crystalline structures corresponding to the phases Al, γU, UAl_3, UAl_4, and $Al_{20}Mo_2U$ were identified by XRD using conventional diffractometer. γU and Al phases correspond to U(Mo,Pt) alloy and Al couple components, respectively. The binary phases UAl_3, UAl_4 and the ternary compound $Al_{20}Mo_2U$ are associated with the interaction layer, Fig. 5.

Composition measurements made on this interaction layer showed that Pt/U ratio remains as in the original U(Mo,Pt) alloy.

3.2.2. U(Mo,Zr)/Al

Crystalline structures corresponding to the phases Al, γU, αU, UAl_3, UAl_4, $Al_{20}Mo_2U$ and $Al_{43}Mo_4U_6$ were identified by XRD using synchrotron radiation. Al, γU, and αU phases correspond to U(Mo,Zr) alloy and Al couple components respectively, while the binary phases UAl_3, UAl_4 and the ternary compounds $Al_{20}Mo_2U$, $Al_{43}Mo_4U_6$ are associated with the interaction layer (Fig. 6).

Composition measurements made on this interaction layer showed that Zr/U ratio remains as in the original U(Mo,Zr) alloy.

3.2.3. U(Mo,Pt)/Al A356

Crystalline structures corresponding to Al, Si, γU, $U(Al,Si)_3$ and U_3Si_5 phases were identified by XRD using conventional diffractometer. γU phase corresponds to U(Mo,Pt) alloy, Al and Si phases correspond to Al A356. $U(Al,Si)_3$ and U_3Si_5 phases are associated with the interaction layer. Lattice parameters estimation resulted in $a = 0.421$ nm for $U(Al,Si)_3$ and $a = 0.393$ nm and $c = 0.403$ nm for U_3Si_5 phase (Fig. 7).

Composition measurements made in this interaction layer are plotted in Fig. 8. A Gibbs triangle diagram was chosen to represent the isothermal section at 550 °C of the pseudo-ternary (U + Mo + Pt)-Al–Si system. XRD results were also added to Fig. 8.

Starting from the Al corner, a first set of composition measurements are linearly spread between pure Al and a concentration value about 50 at.%Al and 25 at.%Si (circled). Based on the XRD

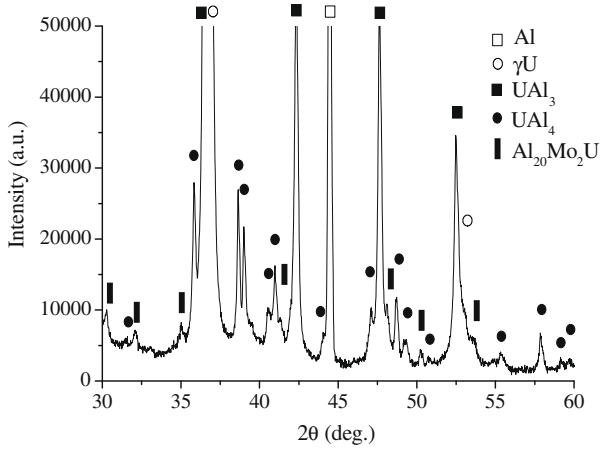

Fig. 5. Sample *II*. 580 °C-2 h. Phase identification in U(Mo,Pt)/Al diffusion couple. Full symbols correspond to the phases associated with the interaction layer. XRD with conventional diffractometer.

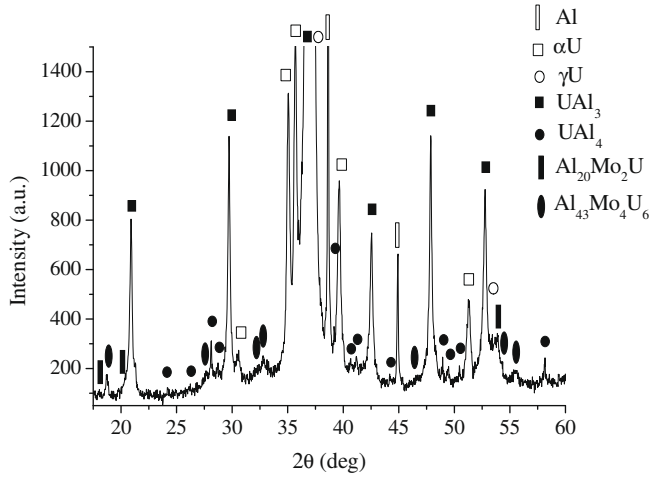

Fig. 6. Sample *VI*. 550 °C-1.5 h. Phase identification in U(Mo,Zr)/Al diffusion couple. Full symbols correspond to the phases associated with the interaction layer. XRD with synchrotron radiation.

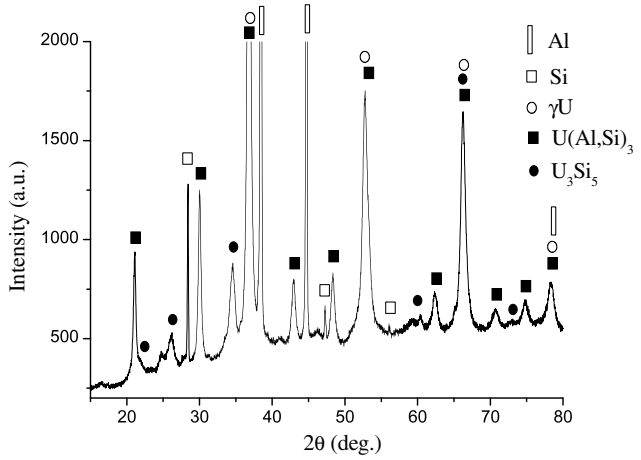

Fig. 7. Sample *IV*. 550 °C-1.5 h. Phase identification in U(Mo,Pt)/Al A356 diffusion couple. Full symbols correspond to the phases associated with the interaction layer. XRD with conventional diffractometer.

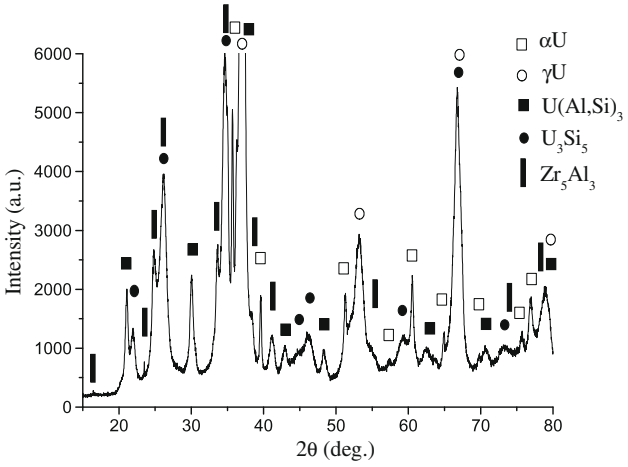

Fig. 9. Sample *VII*, 550 °C-1.5 h. Phase identification in U(Mo,Zr)/Al A356 diffusion couple. Full symbols correspond to the phases associated with the interaction layer. XRD with synchrotron radiation.

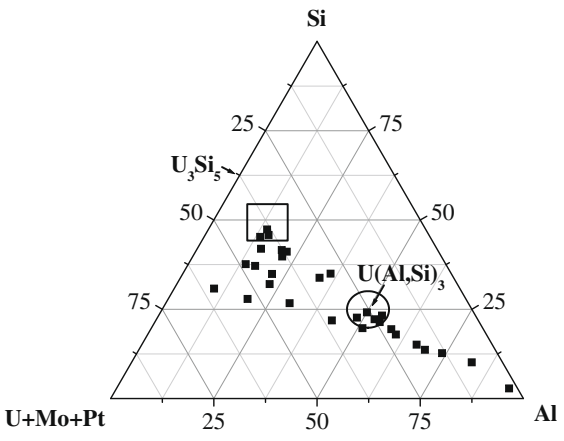

Fig. 8. Sample *III*. 550 °C-1.5 h. Composition measurements in U(Mo,Pt)/Al A356 represented in a pseudo-ternary (U + Mo + Pt)-Al–Si diagram (in at.%). WDS.

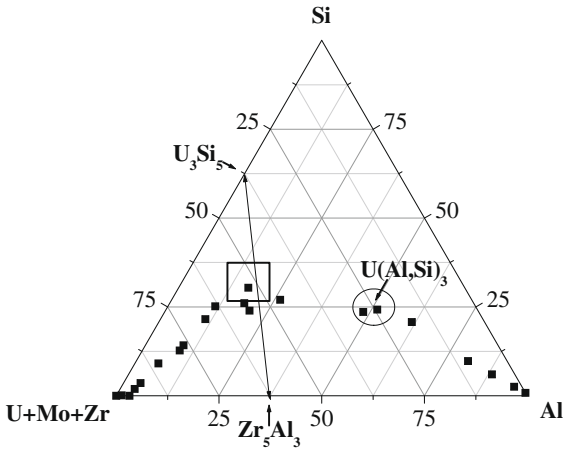

Fig. 10. Sample *V*. 550 °C-1.5 h Composition measurements in U(Mo,Zr)/Al A356 represented in pseudo-ternary (U + Mo + Zr)-Al–Si diagram (in at.%). WDS.

results, each point along this line would correspond to a different proportion of Al + $U(Al,Si)_3$, with 25 at.% Si, phases. A second set of composition measurements could be observed. In this case, all the points are situated into the triangular region determined by: the (U + Mo + Pt) corner, a concentration of about 50 at.%Al and 25 at.%Si (circled) and a concentration of 13 at.%Al and 48 at.%Si (marked with a square). Combining composition and XRD results, the points in this triangular region would correspond to different proportions of γU + U_3Si_5 (with 13 at.%Al) + $U(Al,Si)_3$ (with 25 at.%Si).

3.2.4. U(Mo,Zr)/Al A356

Crystalline structures corresponding to the phases αU, γU, $U(Al,Si)_3$, U_3Si_5 and Zr_5Al_3 (tI32, W_5Si_3 *type*) were identified by XRD using synchrotron radiation, Fig. 9. γU and αU phases correspond to U(Mo,Zr) alloy. $U(Al,Si)_3$, U_3Si_5 and Zr_5Al_3 phases are associated to the interaction layer. Lattice parameter estimation resulted in: $a = 0.421$ nm for $U(Al,Si)_3$ phase, $a = 0.393$ nm and $c = 0.404$ nm for U_3Si_5 phase and $a = 1.075$ nm and $c = 0.537$ nm for Zr_5Al_3 phase.

Composition measurements performed inside the interaction layer are plotted in Fig. 10. The same representation as in Section 3.2.3 was adopted for (U + Mo + Zr)-Al–Si system. XRD results were also added to Fig. 10.

Starting from the Al corner, a first set of composition measurements are linearly spread between pure Al and a concentration value about 50 at.%Al and 25 at.%Si (circled). Based on the phases identified by XRD, each point would correspond to different proportions of Al + $U(Al,Si)_3$, with 25 at.% Si, phases.

Starting from (U + Mo + Zr) corner, a second set of composition measurements could be observed linearly spread between (U + Mo + Zr) corner and a concentration of 17 at.%Al and 30 at.%Si (marked with a square). According to XRD results, this concentration could be explained as a fixed proportion of $U_3Si_5 + Zr_5Al_3$. Then, this second set of points could represent different proportions of γU phase (and or αU) + ($U_3Si_5 + Zr_5Al_3$).

4. Discussion

Additions of Zr or Pt to U(Mo) and Si to Al are studied in this paper to evaluate possible effects on interaction layer characteristics respect to the well known interdiffusion between U(Mo) and pure Al [9–13].

Crystallographic state of U(Mo) alloy has to be taken into account because it affects the interaction layer morphology and phases present in it [10,13,14,23]. In this sense, the addition of Pt or Zr to U(Mo) showed different effects: 0.9 wt.%Pt was enough

Table 2
Effect of Zr on interaction layer thickness in multicouple *V*.

Diffusion couple	Reduction (%)
U–Mo/Al vs. U–Mo–Zr/Al	29
U–Mo/Al A356 vs. U–Mo–Zr/Al A356	33

Table 3
Effect of Si on interaction layer thickness in multicouple *V*.

Diffusion couple	Reduction (%)
U–Mo/Al vs. U–Mo/Al A356	94
U–Mo–Zr/Al vs. U–Mo–Zr/Al A356	94

Table 4
Combined effect of Zr and Si on interaction layer thickness in multicouple *V*.

Diffusion couple	Reduction (%)
U–Mo/Al vs. U–Mo–Zr/Al A356	96

to retain γU phase after 1.5 h at 550 °C meanwhile 1 wt.%Zr enhanced the decomposition process. Even when decomposition in the U-base alloys had occurred, the presence of Si in Al avoided the abrupt growing of the interaction layer. The first observation of this Si effect was presented in [16] for a diffusion couple U–Mo/Al A356 heat treated at 550 °C. In the present work it has been corroborated for U(Mo) and extended to U(Mo,Zr).

In Ref. [23], Zr additions to U(Mo) and Si additions to Al are investigated employing diffusion couple tests. Authors conclude that Zr and Si have similar effects on reducing the interaction layer growth and also remark that Zr is most effective in combination with Si added to Al. Tables 2–4 summarize our results which were obtained from a single sample (i.e. same experimental conditions). As it can be seen, our results showed the same tendency reported in Ref. [23]. Results presented for sample *I* in Section 3.1, show that Pt added to U(Mo) also reduces the width of the interaction layer.

In the diffusion couple U(Mo,Pt)/Al, crystalline structures of the phases that form the interaction layer are the same reported in the literature for γU(Mo)/Al [10,13], meaning that Pt added to U(Mo) does not modify the components inside interaction layer. Same conclusion can be drawn for U(Mo,Zr) with pure Al. In this case the presence of UAl_4 together with $Al_{20}Mo_2U$ let us to infer that the interaction layer started to be formed while U(Mo,Zr) alloy was still in γU phase remaining in this state during some time. The presence of the ternary compound $Al_{43}Mo_4U_6$ indicates that γU phase decomposition occurred while the interdiffusion was still taking place. The binary phase UAl_3 has grown at any of both stages.

On the other hand, other phases are identified when Al A356 alloy is used (samples *IV* and *VII*). $U(Al,Si)_3$ and U_3Si_5 were identified as the phases containing the Si migrated to the interaction layer. These two phases are the same already reported in similar diffusion couples U(Mo)/Al(Si) presented in [14,18]. According to the correlation $U(Al,Si)_3$ lattice parameter vs. Si concentration in this phase, [25], the value $a = 0.421$ nm estimated by XRD in this work, would correspond to ~25 at.% Si. An excellent agreement was found for both samples between this value and the Si concentration extrapolated from WDS measurements. U_3Si_5 phase was identified with increased lattice parameters respect to the original ones ($a = 0.389$ nm and $c = 0.402$ nm), for both samples. This increase in the cell volume is very similar to values reported in [14,18]. In [25] it has been reported that '*the crystalline structure of this phase is a defect type and a ternary element (e.g. Al) could either enter an empty lattice site or displace Si atom*'. Based on this and on the fact that 13 at.%Al was measured in diffusion couple U(Mo,Pt)/Al A356, a possible explanation could be that the presence of Al in this phase is responsible for the cell volume increment mentioned above. Unfortunately there is no literature data available from which to obtain the correlation between lattice parameter vs Al content in the phase U_3Si_5.

In the diffusion couple U(Mo,Zr)/Al A356 (sample *VII*), Zr_5Al_3 phase (which does not contain Si), was also identified as part of the interaction layer. Notice that this phase was not found in the diffusion couple U(Mo,Zr)/Al (sample *VI*). Several works suggest that UAl_3 phase could accept an important amount of Zr in solution and that a small amount of Si in this phase strongly reduced that solubility [26,27]. Based on this, it is proposed that in the diffusion couple U(Mo,Zr)/Al (sample *VI*), Zr could be in solution in UAl_3 phase meanwhile in the diffusion couple U(Mo,Zr)/Al A356 (sample *VII*) Zr forms a new phase (i.e. Zr_5Al_3) due to the presence of Si in $U(Al,Si)_3$ phase.

As observed in this work and in [10,13,14], it is well known that when pure Al or Al 6061 is used, $Al_{43}Mo_4U_6$ is identified in the interaction layer only when irregular interfaces are formed due to the decomposition of γU phase in the U-base alloy and the enhanced diffusion of Al through colonies (αU + γ′U) with lamellar cellular-like morphology (see Fig. 3). Nevertheless, this ternary compound is not identified when Al A356 is used although an important percentage of decomposition was observed on U(Mo,Zr). Considering besides that interaction layer did not show irregular interfaces, any of the phases that formed it, in this case, could be responsible for all of this.

5. Conclusions

A complete characterization of the interaction layers grown by interdiffusion between U–7 wt.%Mo–0.9 wt.%Pt/Al at 580 °C and U–7 wt.%Mo–0.9 wt.%Pt/Al A356 alloy; U–7 wt.%Mo–1 wt.%Zr/Al and U–7 wt.%Mo–1 wt.%Zr/Al A356 alloy at 550 °C was achieved. Results can be summarized as follows:

In U–7 wt.%Mo–0.9 wt.%Pt/Al diffusion couple, the interaction layer is formed by the binary phases UAl_3, UAl_4 and the ternary compound $Al_{20}Mo_2U$.

In U–7 wt.%Mo–1 wt.%Zr/Al, the interaction layer is formed by the binary phases UAl_3 and UAl_4 and the ternary compounds $Al_{20}Mo_2U$ and $Al_{43}Mo_4U_6$.

In U–7 wt.%Mo–0.9 wt.%Pt/Al A356 alloy, the interaction layer is formed by $U(Al,Si)_3$ with 25 at.%Si and U_3Si_5 phase with an increase in the unit cell volume which could be associated to the Al solubility in this phase.

In U–7 wt.%Mo–1 wt.%Zr/Al A356 couple, the interaction layer is formed by $U(Al,Si)_3$ with 25 at.%Si, the U_3Si_5 phase (also with a larger unit cell volume) and Zr_5Al_3 phase.

XRD with synchrotron radiation was a key technique in the identification of Zr_5Al_3 phase.

Acknowledgements

The authors want to thank the technical staff of Dto Materiales, (GIDAT, GAEN, CNEA) for their support and Roosevelt Droppa Jr. from LNLS staff for training in synchrotron radiation equipment. This work was partially financed by Project PICT 12-11186, Agencia de Promoción Cientifica y Tecnológica (Argentina), PIP 5062 CONICET (Argentina) and Project D12A-XRD1·# 5747/06 – Brazilian Syncrotron Light Laboratory –LNLS (Brazil).

References

[1] M.K. Meyer, G.L. Hofman, S.L. Hayes, C.R. Clark, T.C. Wiencek, J.L. Snelgrove, R.V. Starin, K.H. Kim, J. Nucl. Mater. 304 (2002) 221–236.

[2] J.L. Snelgrove, G.L. Hofman, M.K. Meyer, C.L. Trybus, T.C. Wiencek, Nucl. Eng. Des. 178 (1997) 119–126.
[3] A. Leenaers, S. Van den Berghe, E. Koonen, C. Jarousse, F. Huet, M. Trotabas, M. Boyard, S. Guillot, L. Sannen, M. Verwerft, J. Nucl. Mater. 335 (2004) 39–47.
[4] G.L. Hofman, M.R. Finlay, Y.S. Kim, in: Proceedings of the XXVI RERTR International Meeting, November 7–12, 2004, Vienna, Austria.
[5] D.F. Sears, K.T. Conlon, J. Manson, A. Davidson, C. Buchnan, in: Transaction 10th International Topical Meeting ENS RRFM, April 30–May 3, 2006, Sofia, Bulgaria.
[6] V. Popov, V. Khmelevsky, A. Lukichev, O. Golosov, in: Transaction 9th International Topical Meeting ENS RRFM, April 10–13, 2005, Budapest, Hungary.
[7] J.M. Park, H.J. Ryu, Y.S. Lee, B.O. Yoo, Y.H. Jung, C.K. Kim, Y.S. Kim, in: Transaction 12th International Topical Meeting ENS RRFM, March 2–5, 2008, Hamburg, Germany.
[8] S. Van den Berghe, W. Van Renterghem, A. Leenaers, J. Nucl. Mater. 375 (2008) 340–346.
[9] H.J. Ryu, Y.S. Han, J.M. Park, S.D. Park, C.K. Kim, J. Nucl. Mater. 321 (2003) 210–220.
[10] M. Mirandou, S. Balart, M. Ortiz, M. Granovsky, J. Nucl. Mater. 323 (2003) 29–35.
[11] F. Mazaudier, C. Proye, F. Hodaj, J. Nucl. Mater. 377 (2008) 476–485.
[12] E. Perez, N. Hotaling, A. Ewh, D.D. Keiser, Y.H. Sohn, Defect Diffus. 266 (2007) 149–156.
[13] H. Palancher, P. Martin, V. Nassif, R. Tucoulou, O. Proux, J.L. Hazemann, O. Tougait, E. Lahéra, F. Mazaudier, C. Valot, S. Dubois, J. Appl. Crystallogr. 40 (2007) 1064–1075.
[14] M. Mirandou, S. Aricó, S. Balart, L. Gribaudo, Mater. Charact. 60 (2009) 888–893.
[15] R.J. Van Thyne, D.J. McPherson, Trans. ASM 49 (1957) 576–597.
[16] M. Mirandou, M. Granovsky, M. Ortiz, S. Balart, S. Aricó, L. Gribaudo, in: Proceedings of the XXVI RERTR International Meeting, November 7–12, 2004, Vienna, Austria.
[17] Y.S. Kim, G.L. Hofman, H.J. Ryu, J. Rest, in: Proceedings of the XXVII RERTR International Meeting, November 6–11, 2005, Boston, Mass., USA.
[18] M. Mirandou, S. Aricó, M. Rosenbusch, M. Ortiz, S. Balart, L. Gribaudo, J. Nucl. Mater. 384 (2009) 268–273.
[19] C. Komar Varela, M. Mirandou, S. Aricó, S. Balart, L. Gribaudo, in: 11th International Topical Meeting ENS RRFM-IGORR, March 11–15, 2007, Lyon, France.
[20] M. Cornen, F. Mazaudier, X. Iltis, M. Rodier, S. Dubois, P. Lemoine, in: 11th International Topical Meeting ENS RRFM-IGORR, March 11–15, 2007, Lyon, France.
[21] C. Komar Varela, M. Mirandou, S. Aricó, S. Balart, L. Gribaudo, in: Proceedings of the XXIX RERTR International Meeting, September 23–27, 2007, Prague, Czech Republic.
[22] D. Keiser Jr., Defect Diffus. Forum 266 (2007) 131–148.
[23] J.M. Park, H.J. Ryu, S.J. Oh, D.B. Lee, C.K. Kim, Y.S. Kim, G.L. Hofman, J. Nucl. Mater. 374 3 (2008) 422–430.
[24] W. Kraus, G. Nolze, U. Müller, PowderCell 2.3. – Pulverdiffraktogramme aus Einkristalldaten und Anpassung experimenteller Beugungsaufnahmen, 2000, <http://www.bam.de/de/service/publikationen/powder_cell_a.htm>.
[25] A.E. Dwight, Report Specification No. ANL-82-14, 1982, pp. 1–39.
[26] L.M. Pizarro, P.R. Alonso, G.H. Rubiolo, J. Nucl. Mater. 392 (2009) 70–77.
[27] G. Petzow, H.E. Exner, A.K. Chakraborty, J. Nucl. Mater. 25 (1968) 1–15.